SCIENCE CHINA
Earth Sciences

•ARTICLE•

https://doi.org/10.1007/s11430-024-1580-0

The 2023 summer drought and high temperatures turned the East China Sea off the Changjiang estuary from a CO_2 sink to a CO_2 source

Yi XU[1], Dezhi BU[1], Xianghui GUO[1,2*], Shiping LEI[1], Yi YANG[1] & Kuanbo ZHOU[1]

[1] State Key Laboratory of Marine Environmental Science, College of Ocean and Earth Sciences, Xiamen University, Xiamen 361102, China
[2] Fujian Provincial Key Laboratory for Coastal Ecology and Environmental Studies, Xiamen University, Xiamen 361102, China

Received July 14, 2024; revised April 26, 2025; accepted May 7, 2025; published online May 29, 2025

Abstract This study reports the surface water partial pressure of CO_2 ($p$$CO_2$) and air-sea CO_2 fluxes on the East China Sea shelf off the Changjiang estuary in August 2023. Surface water $p$$CO_2$ ranged from 110 μatm to 910 μatm with an average value of 427±154 μatm. Air-sea CO_2 fluxes in the surveyed area ranged from −20.6 mmol m^{-2} d^{-1} to 35.9 mmol m^{-2} d^{-1} and averaged 3.0±8.9 mmol m^{-2} d^{-1} (a moderate source), which was contrary to this region generally being a CO_2 sink during summer. Changjiang discharge played a key role in regulating surface water $p$$CO_2$; the decreased Changjiang discharge in August 2023 increased surface water $p$$CO_2$ on the adjacent inner shelf substantially, and the high sea surface temperature further elevated the surface water $p$$CO_2$. The combined effect of drought and high temperatures in August 2023 turned the study area from a CO_2 sink to a CO_2 source. Under the context of global change, climate events such as floods, droughts and heatwaves occur more frequently, which will continue to add more complexity to CO_2 sink/source evaluations in large river-dominated marginal seas and suggest further research is needed.

Keywords East China Sea shelf, Changjiang estuary, Summer drought, $p$$CO_2$, Air-sea CO_2 flux, CO_2 source, Discharge

Citation: Xu Y, Bu D, Guo X, Lei S, Yang Y, Zhou K. 2025. The 2023 summer drought and high temperatures turned the East China Sea off the Changjiang estuary from a CO_2 sink to a CO_2 source. Science China Earth Sciences, 68, https://doi.org/10.1007/s11430-024-1580-0

1. Introduction

Air-sea CO_2 fluxes in marginal seas are an important component of the ocean's carbon cycle (Laruelle et al., 2018; Dai et al., 2022). However, there are still challenges in reliably assessing the air-sea CO_2 fluxes in individual coastal systems (Dai et al., 2022). CO_2 dynamics in marginal seas are often influenced by complex processes such as riverine discharge (Huang et al., 2015), coastal upwelling (Hales et al., 2005), dynamic cross-shelf and/or shelf-ocean exchanges (Wang et al., 2013), and intrinsic biogeochemical cycling. Therefore, variations in river inputs and seasonal asymmetry of biogeochemical processes and episodic weather events (Fassbender et al., 2018; Wu et al., 2021) add more complexity to air-sea CO_2 flux estimates. Reliably estimating regional air-sea CO_2 fluxes is important as it not only affects global CO_2 flux estimates but also improves our modeling capabilities of the coastal ocean carbon cycle.

The East China Sea has a large shelf that receives freshwater inputs from a major world river, the Changjiang (Yangtze River). Additionally, it has dynamic exchange at its eastern boundary with the Kuroshio, a major western ocean boundary current (Chen and Wang, 1999). Studies of air-sea CO_2 fluxes in the East China Sea began in the 1990s (Tsunogai et al., 1997, 1999; Wang et al., 2000; Hu and Yang, 2001). Tsunogai et al. (1999) found that the East China Sea is a strong CO_2 sink of ~8 mmol m^{-2} d^{-1} (35 gC m^{-2} yr^{-1}), mainly based on data collected in summer, fall and winter

* Corresponding author (email: xhguo@xmu.edu.cn)

along the PN line (a line connecting 31.4°N, 123.0°E on the inner shelf off the Changjiang estuary and 27.5°N, 128.4°E west of Amami Islands). Hu and Yang (2001) suggested that the East China Sea shelf is a weak CO_2 sink based on observations during all four seasons of the year.

Within the last two decades, more studies have revealed the spatial and seasonal variability of the air-sea CO_2 fluxes and their major driving factors, and have achieved a consensus that the East China Sea is a strong CO_2 sink annually (Shim et al., 2007; Zhai and Dai, 2009; Chou et al., 2009, 2011; Tseng et al., 2011, 2014; Kim et al., 2013; Guo et al., 2015). Among these studies, Tseng et al. (2011, 2014) demonstrated that Changjiang discharge plays a dominant role in controlling the CO_2 sink capacity of the East China Sea shelf. Guo et al. (2015) suggested that seasonal changes in the surface water partial pressure of CO_2 ($p$$CO_2$) vary in different sub-regions of the East China Sea. Although Changjiang discharge has a large influence on the surface water $p$$CO_2$ in the inshore sub-region and the Changjiang plume, the surface water $p$$CO_2$ of the outer shelf is dominated by temperature variability (Guo et al., 2015). Yu et al. (2023) showed the long-term (2003–2019) pattern of air-sea CO_2 fluxes in the East China Sea based on reconstructed $p$$CO_2$ data, which indicates its CO_2 sink capacity has been increasing. Additionally, conspicuous inter-annual variabilities in air-sea CO_2 fluxes were also observed (Guo et al., 2015; Yu et al., 2023), but the pattern and driving factors of these variations are still largely unknown. Yu et al. (2024) found that the CO_2 sink capacity of the East China Sea in 2022 was reduced due to a drought and heatwave.

As opposed to the general consensus of the East China Sea off the Changjiang estuary being a CO_2 sink in summer, this study presents field observations of it acting as a CO_2 source in August 2023, a rare phenomenon. We demonstrate that the combined effects of lowered Changjiang discharge and high temperatures in August 2023 were responsible for it turning from a CO_2 sink to a CO_2 source.

2. Materials and methods

2.1 Study area

The East China Sea is located in the temperate and subtropical northwestern Pacific, covering a surface area of 1.25×10^6 km^2 with >70% being the continental shelf shallower than 200 m (Figure 1). The Changjiang inputs 940 km^3 of freshwater (Dai and Trenberth, 2002), 300×10^4 t of N, 8×10^4 t of P, and 100×10^4 t of Si into the East China Sea annually (Zhang et al., 2007; Gao et al., 2009; Li et al., 2014), with fluxes peaking in summer.

The East China Sea is connected to the Yellow Sea in the north and the South China Sea in the south through the Taiwan Strait (Figure 1). The East China Sea is located in a

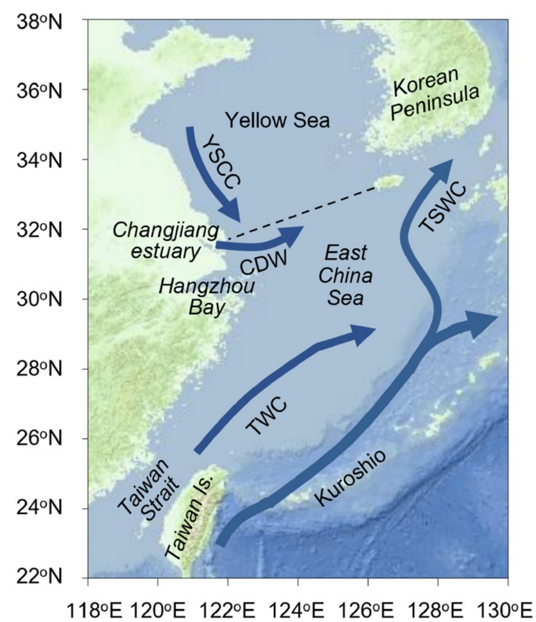

Figure 1 Topographic map of the East China Sea shelf adjacent to the Changjiang estuary with the major surface currents in summer shown. CDW is Changjiang Diluted Water; YSCC is the Yellow Sea Coastal Current; TWC is the Taiwan Warm Current; TSWC is the Tsushima Warm Current.

region modulated by the East Asian monsoon, with a strong northeastern monsoon dominating in winter and a relatively weak southwestern monsoon dominating in summer. The Changjiang plume flows northeastward in summer and southwestward along the China mainland coast in winter (Lee and Chao, 2003). On the northern East China Sea shelf, the Yellow Sea Coastal Current flows southward year-round, which brings coastal Yellow Sea water to the coastal East China Sea except in summer during the influence of the southwest monsoon (Yuan et al., 2017; Liu et al., 2021). In the offshore area, the northward flowing Kuroshio, characterized by high temperatures and salinities, follows along the ~200 m isobath beyond the shelf break (Lee and Chao, 2003; Liu et al., 2021). The Kuroshio and Changjiang plume mainly drive water mixing on the East China Sea shelf (Yang et al., 2011).

The sea surface temperature (SST) in the East China Sea is lower in winter and early spring, and higher in summer and early fall (Guo et al., 2015). In general, primary productivity on the East China Sea shelf is also lower in winter due to the low temperatures, but higher during warm seasons (Gong et al., 2011). On the inner East China Sea shelf, freshwater discharge and primary productivity mainly control the surface water $p$$CO_2$ and air-sea CO_2 fluxes (Tseng et al., 2014; Guo et al., 2015). High productivity on the shelf in summer coincides with strong stratification, with low $p$$CO_2$ and high dissolved oxygen (DO) in the surface water but high $p$$CO_2$ and low DO in the subsurface and bottom waters (Chou et al., 2009).

2.2 Sampling and analysis

A field survey was conducted from August 14–22 of 2023 onboard the R/V Yanping II. During the cruise, SST, sea surface salinity (SSS), surface water pCO_2, and DO were measured continuously.

Surface water pCO_2 was measured continuously with a non-dispersive infrared spectrometer (Li-Cor® 7000) integrated with a homemade continuous measurement system. The system was described by Zhai et al. (2005, 2013), Zhai and Dai (2009). Surface water was continuously pumped from 3–5 m depth and the CO_2 mole fraction (xCO_2) was determined after air-water equilibration.

DO was measured with a YSI EXO multiple-sensor sonde integrated into the underway system. Discrete water samples were taken for DO measurements, fixed with Winker repeats (Carpenter, 1965) and measured spectrophotometrically at 466 nm onboard within 4 h of sampling (Labasque et al., 2004) (see details in Lei et al. (2024)). The sensor-measured DO was calibrated with the spectrophotometrically measured DO data.

Wind speed and barometric pressure were measured with an R.M. Young 05106 marine wind sensor and a 61302V barometer, which were integrated with a 32500 magnetic compass. The sensors were located at ~10 m above the sea surface. The precision of wind speed and barometric pressure measurements was ±0.3 m s^{-1} and ±3 hPa, respectively.

2.3 Data processing

Water pCO_2 at the temperature in the equilibrator (pCO_2^{Eq}) was calculated from the xCO_2 in dry air in the equilibrator and the pressure in the equilibrator (P_{Eq}) after correcting for the vapor pressure (P_{H_2O}) of water at 100% relative humidity (Weiss and Price, 1980):

$$pCO_2^{Eq} = \left(P_{Eq} - P_{H_2O}\right) xCO_2. \quad (1)$$

Atmospheric pCO_2 was calculated similarly with atmospheric xCO_2 and the barometric pressure, using a formula similar to eq. (1). Monthly atmospheric xCO_2 in August 2023 over the Tae-ahn Peninsula (36.7376°N, 126.1328°E, http://www.esrl.noaa.gov/gmd/dv/site) was adopted in the atmospheric pCO_2 calculation.

Water pCO_2^{Eq} obtained from eq. (1) was corrected to pCO_2 at SST (*in situ* pCO_2, or pCO_2 hereafter) using the empirical formula of Takahashi et al. (1993), where t is the temperature in the equilibrator.

$$pCO_2 = pCO_2^{Eq} e^{0.0423(SST-t)}. \quad (2)$$

The air-sea CO_2 flux (FCO_2) was calculated using the following formula:

$$FCO_2 = k \times s \times \Delta pCO_2, \quad (3)$$

where s is the solubility coefficient of CO_2 (Weiss, 1974), ΔpCO_2 is the pCO_2 difference between the surface water and the atmosphere, and k is the CO_2 transfer velocity. As defined here, a positive flux indicates CO_2 evasion from the sea to the atmosphere. k was parameterized using the empirical function of Sweeney et al. (2007) (k (S07)):

$$k(\mathrm{S07}) = 0.27U_{10}^2 \times \left(\frac{Sc}{660}\right)^{-0.5}, \quad (4)$$

where U_{10} is the monthly mean wind speed at 10 m above sea level, and Sc is the Schmidt number at *in situ* temperatures of surface seawater (Wanninkhof, 1992).

Surface water pCO_2 normalized to a constant temperature of 29°C (average SST during the August 2023 cruise), $NpCO_2$ at 29°C, was calculated following Takahashi et al. (1993):

$$NpCO_2(29°C) = pCO_2 e^{0.0423(29-SST)}. \quad (5)$$

As water pCO_2 shows a relationship with water temperature at a rate of 4.23% °C^{-1} (Takahashi et al., 1993), $NpCO_2$ can reflect non-temperature influences on surface water pCO_2, such as terrestrial inputs, biological processes, and water mixing.

DO saturation (in %) was defined as the ratio of measured DO concentration to the saturated DO concentration, the latter of which was calculated according to the empirical formula of Benson and Krause (1984).

The influence of SST on surface water pCO_2 was calculated using the 4.23% °C^{-1} relationship (Takahashi et al., 1993). To estimate the influence of drought (low Changjiang discharge) on surface water pCO_2, we used the relationship of $NpCO_2$ (at 25°C) with the Changjiang discharge (in 10^3 m^3 s^{-1}, eq. (6), Tseng et al., 2014), which was developed based on a 14-year field observation dataset in the Changjiang plume.

$$NpCO_2(25°C) = -2.71 \times \text{discharge} + 427. \quad (6)$$

$NpCO_2$ (at 25°C, in µatm, 1 atm=1.01325×10^5 Pa) was then normalized to the *in situ* SST in August 2023 or other SSTs which were discussed with the 4.23% °C^{-1} relationship (Takahashi et al., 1993).

3. Results and discussion

3.1 Hydrologic setting

The long-term average monthly freshwater discharge from the Changjiang ranges from 1.4×10^4 m^3 s^{-1} to 4.9×10^4 m^3 s^{-1}, with low discharge in winter and high discharge in summer. However, the lower Changjiang drainage basin was dry from spring to summer in 2023, and monthly average freshwater discharge from June to August ranged from 2.6×10^4 m^3 s^{-1} to 3.0×10^4 m^3 s^{-1}, ~60% of the long-term monthly averages (Figure 2).

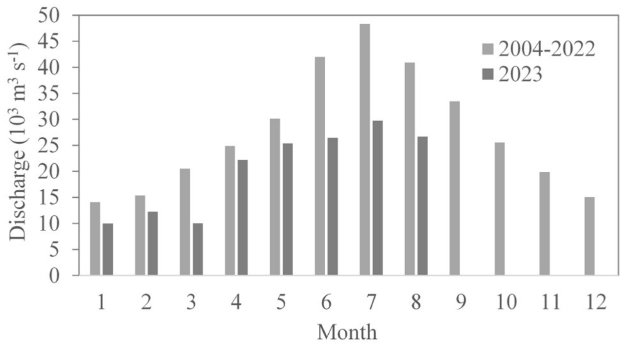

Figure 2 Monthly average freshwater discharge of the Changjiang in 2023, and the long-term average (2004–2022) at the Datong gauge station. The data are from the Ministry of Water Resources of the People's Republic of China (http://xxfb.hydroinfo.gov.cn/).

SSTs ranged from 25.6°C to 31.0°C, and were >28.0°C in most of the surveyed areas (Figure 3a). Low temperatures were observed at the southwestern corner of the study area, and high temperatures were observed in the offshore area. SSS ranged from 7.8 to 34.1, with low salinities in the inshore area and increasing offshore. Waters with SSS<32.0 covered only ~1/3 of the surveyed area (Figure 3b).

3.2 Distributions of pCO$_2$, DO and air-sea CO$_2$ fluxes

Surface water pCO$_2$ ranged from 110 μatm to 910 μatm, and its spatial distribution was patchy. Low pCO$_2$ (<360 μatm) was generally observed in the area off the Changjiang estuary mouth and off Hangzhou Bay, and high pCO$_2$ (>400 μatm) was observed in the southeastern offshore area. However, the most inshore zones just off the Changjiang estuary mouth and Hangzhou Bay were characterized by very high pCO$_2$ (>500 μatm) (Figure 3c). Average surface water pCO$_2$ across the study region was 427±154 μatm. Normalized to the same temperature (29°C), NpCO$_2$ values showed a similar spatial pattern to *in situ* pCO$_2$, but with less variability (Figure 3d). Atmospheric pCO$_2$ ranged from 394 μatm to 404 μatm, showing much less spatial variability than that of the surface water.

DO saturation ranged from 71% to 250%, and its spatial distribution showed the opposite pattern to surface water pCO$_2$ values. In the low pCO$_2$ area off the Changjiang estuary, DO saturation was >150%; in the high-pCO$_2$ inshore-most water, DO saturation was <90%. In the southeastern offshore area, DO saturation was ~100% (Figure 3e).

Air-sea CO$_2$ fluxes ranged from −20.6 mmol m^{-2} d^{-1} (short-term CO$_2$ sink) to 35.9 mmol m^{-2} d^{-1} (short-term CO$_2$ source) during the survey. Strong CO$_2$ sources (air-sea CO$_2$ flux >10 mmol m^{-2} d^{-1}) were located in the very inshore waters off the Changjiang estuary mouth and off Hangzhou Bay, while strong CO$_2$ sinks (air-sea CO$_2$ flux <−5 mmol m^{-2} d^{-1}) were distributed heterogeneously in the low-pCO$_2$ zones (Figure 3f). The southeastern offshore area was a weak to moderate CO$_2$ source (air-sea CO$_2$ flux was 0–5 mmol m^{-2} d^{-1}). The average air-sea CO$_2$ flux of the surveyed area was 3.0±8.9 mmol m^{-2} d^{-1}, indicating that the region as a whole was a weak to moderate CO$_2$ source at the time of the survey.

3.3 Major factors influencing surface water pCO$_2$

As SST has a large influence on surface water pCO$_2$, and because SST showed large spatial and temporal variability, it's difficult to determine a thermodynamic pCO$_2$ range. We thus used a temperature-normalized pCO$_2$ (NpCO$_2$) range in the zone where temperature dominates the surface water pCO$_2$ values, and then normalized the NpCO$_2$ to SST to get

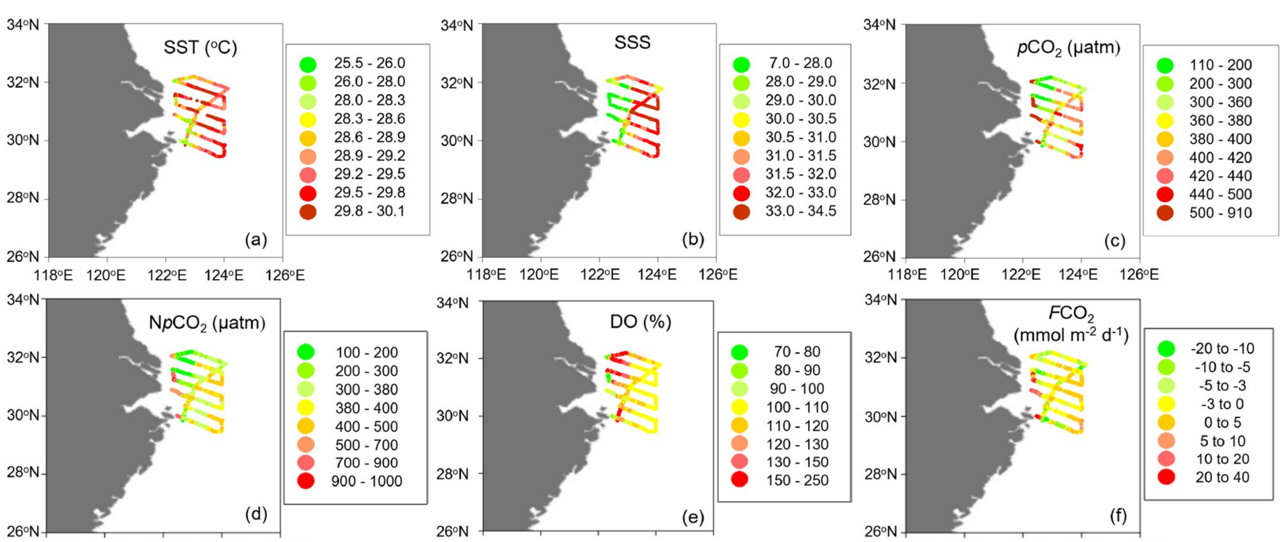

Figure 3 Spatial distributions of SST, SSS, surface water pCO$_2$, NpCO$_2$, DO saturation (DO%) and air-sea CO$_2$ flux (FCO$_2$).

the *in situ* thermodynamic pCO_2 range. Taking the $NpCO_2$ minimum and maximum (at 29°C, 390–440 μatm) in the offshore zone as the thermodynamically controlled $NpCO_2$ lower and upper limits, the thermodynamically controlled pCO_2 limits were determined as $390\times e^{0.0423\times(SST-29)}$ and $440\times e^{0.0423\times(SST-29)}$ μatm (normalized to SST during the cruise, dotted lines in Figure 4a). Most pCO_2 values were higher or lower than the thermodynamically controlled pCO_2 range (Figure 4a), indicating that SST was not the sole factor regulating surface water pCO_2 levels. pCO_2 in the low-salinity inshore-most zone was higher than the upper limit of the thermodynamically controlled pCO_2 (the upper dotted line in Figure 4a), while the low-pCO_2 values were lower than the thermodynamically controlled lower pCO_2 limit (the lower dotted line in Figure 4a). It should be noted that the area with pCO_2 values lower than the thermodynamically controlled lower limit, or within the thermodynamically controlled pCO_2 range, does not suggest a CO_2 sink, as the dynamically controlled pCO_2 range was higher than the atmospheric pCO_2 level over most of the SST range (Figure 4a).

$NpCO_2$ (at 29°C) was high in the inshore-most zone, but the high-$NpCO_2$ area was very limited. For most of the dataset, $NpCO_2$ didn't show a conspicuous relationship with salinity (Figure 4b). Taking the surface water pCO_2 at equilibrium with the atmosphere ($pCO_{2,\ temp}$) as a reference, the difference between the observed surface water pCO_2 and the $pCO_{2,\ temp}$ (pCO_2−$pCO_{2,\ temp}$) is the non-thermodynamically dominated pCO_2 (Zhai et al., 2025).

$$pCO_{2,\,temp} = pCO_{2,\,air}e^{0.0423(SST-29)}, \tag{7}$$

where $pCO_{2,\ air}$ was the average atmospheric pCO_2 (398.7 μatm) at the average SST during the cruise. Therefore, $pCO_{2,\ temp}$ is the assumed water pCO_2 level at *in situ* temperature and equilibrium with the atmosphere.

The results (Figure 4c) were generally consistent with the previous observations. The inshore-most high pCO_2 values were the result of riverine inputs, local biogeochemically produced CO_2, or the influence of upwelled high-pCO_2 water (Zhai and Dai, 2009; Guo et al., 2021). The low surface water pCO_2 values were induced by phytoplankton CO_2 uptake (Zhai and Dai, 2009; Guo et al., 2021). The patchy surface water pCO_2 distribution was the result of the combined influences of multiple processes, including high-pCO_2 estuarine water inputs, biological CO_2 uptake, high-pCO_2 subsurface water mixing, and the heating effect (increasing pCO_2) during the hot summer (Figure 3a, 3c).

3.4 The summer drought and high temperatures turned the East China Sea off the Changjiang estuary from a CO_2 sink to a CO_2 source

Nutrient input fluxes from the Changjiang are dominated by river discharge (Gao et al., 2012; Wang et al., 2019), and

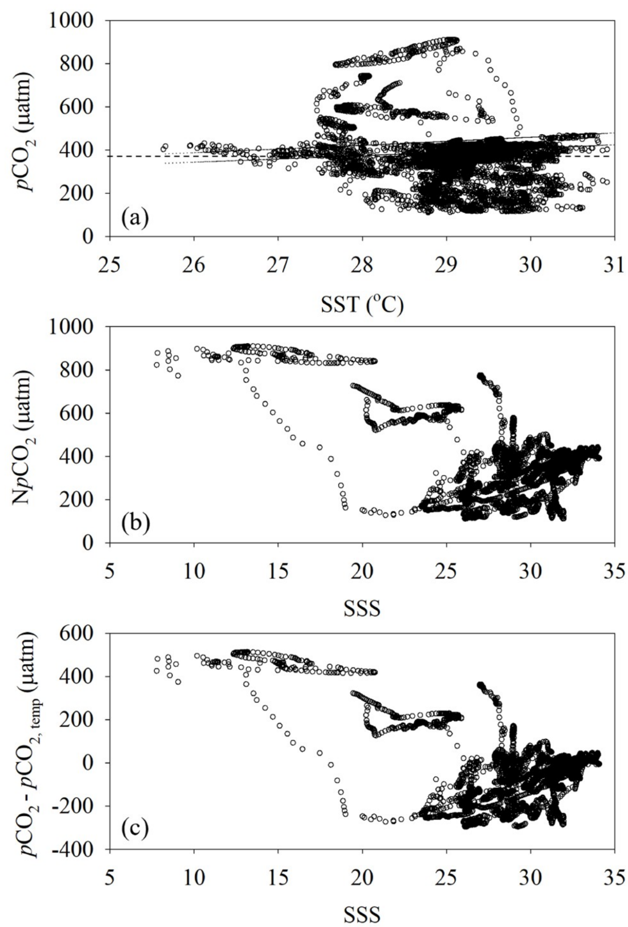

Figure 4 (a) Relationships of surface water pCO_2 with SST; (b) normalized surface water pCO_2 to 29°C ($NpCO_2$) with SSS; (c) pCO_2-pCO_2 (temp) with SSS. The dotted lines in panel a represent $390\times e^{0.0423\times(SST-29)}$ μatm and $440\times e^{0.0423\times(SST-29)}$ μatm, in which 390 μatm and 440 μatm are the lower and upper limits of $NpCO_2$ in the offshore area (with the highest SSS). The horizontal dashed line in panel a shows the average atmospheric pCO_2 level.

Changjiang floods are the major regulator of phytoplankton biomass on the East China Sea shelf (Gong et al., 2011). Therefore, the low discharge from the Changjiang during August 2023 would be expected to result in lower phytoplankton biomass. The chlorophyll a concentration in August 2023 was ~50% of the long-term (2004–2022) monthly average in August (data in the surveyed area shown by the dashed rectangle in Figure 5), and the area of the high-chlorophyll zone in August 2023 was also smaller than the long-term monthly average (Figure 5). Field observation data showed that surface water pCO_2 decreased with increasing chlorophyll a concentrations in the Changjiang plume (Guo et al., 2015). As a result of the lower chlorophyll a concentrations and hence lower phytoplankton CO_2 uptake across most of the study area, surface water pCO_2 in August 2023 should be higher.

The surveyed area as a whole was a short-term CO_2 source in August 2023. This is contrary to the general case in summer; influenced by Changjiang inputs, the Changjiang plume area is typically a CO_2 sink in summer based on data collected from dozens of field surveys (Chou et al., 2009; Tseng et al., 2014; Guo et al., 2015). According to different physical-biogeochemical characteristics, Guo et al. (2015) divided the East China Sea shelf into five domains, and the surveyed area of this study was in Domain I (the solid rectangle in Figure 6). This domain is the Changjiang plume region, and it was a CO_2 sink of 1.6–10.2 mmol m^{-2} d^{-1} during all the summer cruises (Guo et al., 2015). We therefore take observations from the August 2009 cruise as an example to compare to our current dataset. As the surface water pCO_2 might be increasing as a result of increasing atmospheric pCO_2, 28 μatm was added to the surface water pCO_2 data collected during the August 2009 cruise, assuming the surface water pCO_2 was increasing at a rate of 2 μatm yr^{-1} (Guo et al., 2015). The adjusted pCO_2 results are shown in Figure 6b.

Surface water pCO_2 during August 2023 was much higher than in August 2009 (Figure 6). It ranged from 110–910 μatm in the surveyed area of the August 2023 cruise, and pCO_2 in more than half the area was >400 μatm (Figure 6a). The average air-sea CO_2 flux was 3.0 mmol m^{-2} d^{-1}. However, surface water pCO_2 measurements taken during August 2009 that are within the August 2023 surveyed area (dotted rectangle, Figure 6b) were generally <360 μatm, although the inshore-most zone off the Changjiang estuary mouth was still characterized by high pCO_2 (>400 μatm) (Figure 6b). The average air-sea CO_2 flux across all of Domain I during 2009 was −8.4 mmol m^{-2} d^{-1}. Therefore, in 2009 the CO_2 sink strength of waters within the 2023 surveyed area should also have been stronger, as surface water pCO_2 in the southeastern area beyond the surveyed area was relatively high (>400 μatm) (Figure 6b). In summary, this comparison of air-sea CO_2 fluxes during August 2023 and the earlier summer cruises (Tseng et al., 2014; Guo et al., 2015), the case of the studied shelf region being a CO_2 source in August 2023, was contrary to it

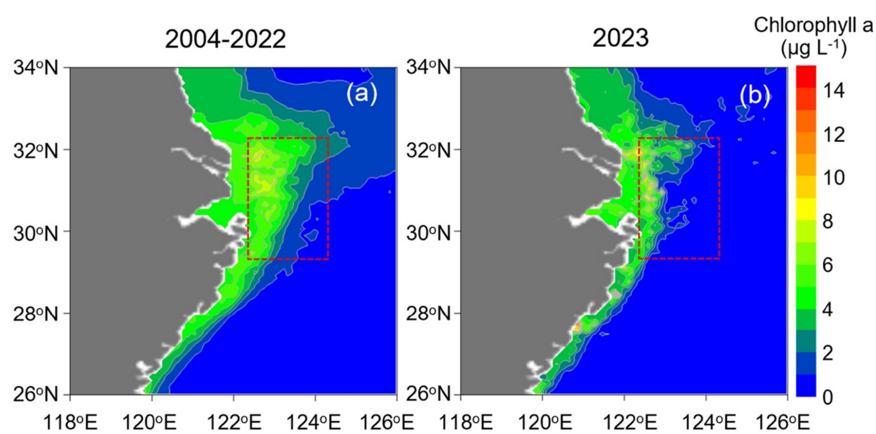

Figure 5 Spatial distribution of long-term monthly average satellite-derived chlorophyll a concentrations in August from 2004–2022 (a) and August 2023 (b) on the East China Sea shelf. Monthly mean chlorophyll a concentrations were obtained from the APDRC (Asia-Pacific Data Research Center) website (http://apdrc.soest.hawaii.edu:80/dods/public_data/satellite_product/MODIS_Aqua/chla_mapped_mon_4km), which were retrieved with the MODIS (Moderate Resolution Imaging Spectroradiometer) onboard the NASA Aqua satellite. The red dashed rectangles indicate the surveyed area during August 2023.

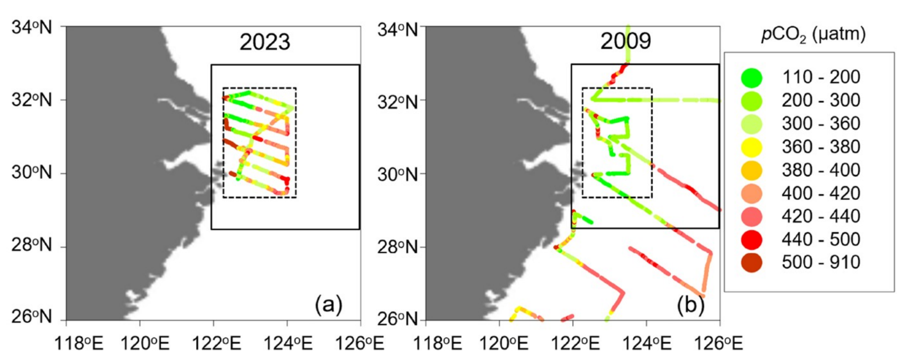

Figure 6 A comparison of surface water pCO_2 values in August 2023 (a) with those from August 2009 (b). The 2009 data are from Guo et al. (2015), and 28 μatm was added to the values so they are comparable with the August 2023 data, assuming that the surface water pCO_2 was increasing at a rate of 2 μatm yr^{-1} (Guo et al., 2015). The dotted rectangles show the surveyed area of the August 2023 cruise, and the solid rectangles show Domain I of Guo et al. (2015).

generally being a CO_2 sink in summer.

14-year field observations showed that the average normalized pCO_2 in the study area is linearly correlated to the Changjiang discharge ($NpCO_2$ at 25°C (in μatm)= −2.71×discharge (in 10^3 m^3 s^{-1})+427) (Tseng et al., 2014). During the August 2023 cruise, the average SST was 29.06°C and the monthly average discharge of the Changjiang was 26.68×10^3 m^3 s^{-1}. Based on these values, the estimated average surface water pCO_2 should be 419 μatm, which is close to the observed average surface water pCO_2 (427 μatm) during the August 2023 cruise. If the long-term (2004–2022) monthly average discharge in August (40.90×10^3 m^3 s^{-1}) is instead adopted, the estimated average surface water pCO_2 would be 373 μatm (Figure 7). Therefore, the decreased Changjiang discharge in August 2023 increased the surface water pCO_2 of the study area substantially.

SST also played an important role in the high surface water pCO_2 in August 2023. The average observed SST (29.06°C) during the August 2023 cruise was higher than during field observations by Tseng et al. (2014) and Guo et al. (2015). From the remote data, SST in the August 2023 surveyed area was ~1°C higher than the long-term (2004–2022) monthly average SST in August (Figure 8). As surface water pCO_2 increases with SST at a rate of 4.23% °C^{-1} (Takahashi et al., 1993), the estimated surface water pCO_2 in August under long-term average Chanjiang discharge and long-term average SST in August would be 357 μatm, which is lower than estimates using August 2023 SST (373 μatm at 29.06°C, Figure 7).

Lowering SST from 29.0°C to 24.0°C, surface water pCO_2 would decrease by 80 μatm to 338 μatm (from 418 μatm) using river discharge rates during August 2023 (Figure 9a). At SST <27.9°C, the average pCO_2 in the surveyed area would be lower than the atmospheric pCO_2 even under the dry conditions (as during August 2023). From 29.0°C to 24.0°C, air-sea CO_2 fluxes decreased from 0.90 mmol m^{-2} d^{-1} (source) to −2.77 mmol m^{-2} d^{-1} (sink) estimated with the same atmospheric pCO_2 and wind speeds during the August 2023 cruise (Figure 9b). Nevertheless, for the long-term (2004–2022) average discharge in August, the surveyed area would be a CO_2 sink even at 30.0°C (Figure 9). Therefore, the combined effects of a summer drought and high temperatures induced the CO_2 source in the surveyed area during August 2023.

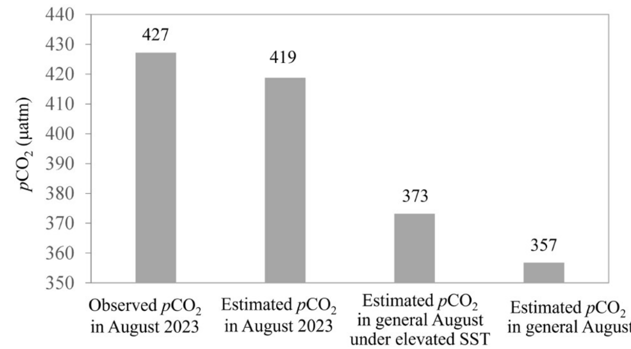

Figure 7 Comparison of the observed and estimated surface water pCO_2 during August 2023, and under long-term monthly Changjiang discharge in August. The numbers in Figure 7 are the pCO_2 values. The estimated surface water pCO_2 was calculated based on the empirical function of surface water pCO_2 with monthly average freshwater discharge of the Changjiang and SST as suggested by Tseng et al. (2014). The estimated pCO_2 in general August under elevated SST was calculated based on the long-term (2004–2022) monthly freshwater discharge in August and SST in August 2023, which was 1°C higher than the long-term monthly average SST in August. The estimated pCO_2 in general August was calculated based on the long-term monthly freshwater discharge and SST in August. The freshwater discharge was measured at the Datong gauge station, and the long-term averages are from 2004–2022. The data were obtained from the Ministry of Water Resources of the People's Republic of China (http://xxfb.hydroinfo.gov.cn/). The long-term (2004–2022) average SST (28.0°C) values were obtained from the APDRC (Asia-Pacific Data Research Center) Public-Access Products website (http://apdrc.soest.hawaii.edu:80/dods/public_data/NOAA_SST/OISST/Monthly_high_res/sst). The NOAA OI.v2.1 SST monthly fields are derived by a linear interpolation of the weekly optimum interpolation (OI) version 2 fields to daily fields, then averaging the daily values over a month.

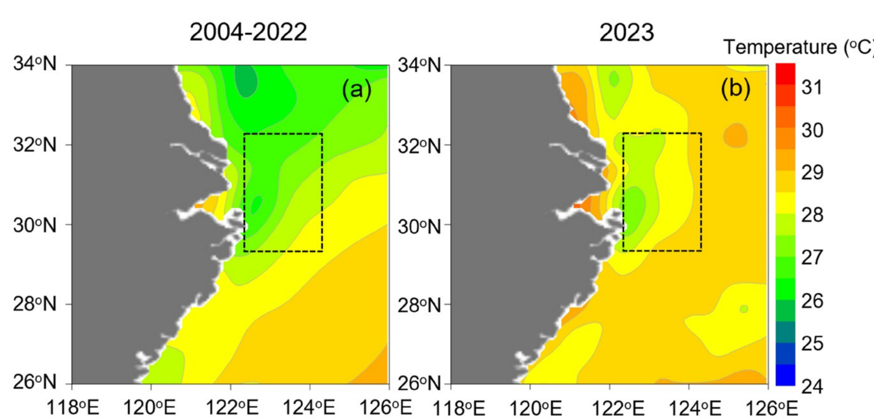

Figure 8 Spatial distribution of monthly average SSTs in August from 2004 to 2022 (a) and August 2023 (b) on the East China Sea shelf. The dotted rectangles show the surveyed area in August 2023. Monthly mean SSTs were obtained from the APDRC (Asia-Pacific Data Research Center) Public-Access Products website (http://apdrc.soest.hawaii.edu:80/dods/public_data/NOAA_SST/OISST/Monthly_high_res/sst). The NOAA OI.v2.1 SST monthly fields are derived by a linear interpolation of the weekly optimum interpolation (OI) version 2 fields to daily fields, then averaging the daily values over a month.

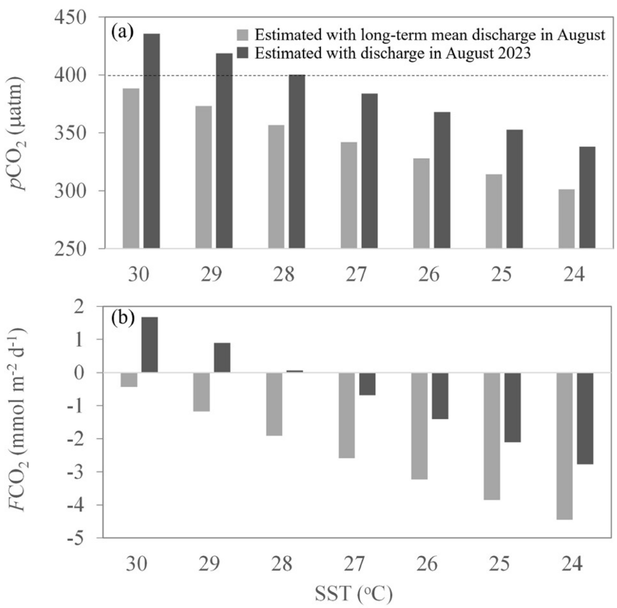

Figure 9 Changes of estimated surface water pCO_2 (a) and air-sea CO_2 fluxes (FCO_2) (b) with SST. The long-term mean discharge in August is the monthly mean discharge in August from 2004–2022. Surface water pCO_2 was estimated with the empirical formula of Tseng et al. (2014) that determines pCO_2 (μatm) with a given Changjiang discharge (10^3 m^3 s^{-1}) and SST (°C). Air-sea CO_2 fluxes were calculated based on the mean wind speed, atmospheric pCO_2, and estimated surface water pCO_2. The dashed line in panel a shows the atmospheric pCO_2 level.

It should be noted that the purpose of the simplified estimation above is not to simulate the accurate air-sea CO_2 fluxes. Instead, it is used to explain why the East China Sea off the Changjiang estuary was a CO_2 source in August 2023, which is contrary to it being a CO_2 sink under typical summer conditions. The combined effects of decreased river discharge and high temperatures turned the study area from a CO_2 sink to a source, which is shown conceptually in Figure 10. In the context of global warming and increasing frequency of extreme weather events, the CO_2 sink/source patterns of coastal seas, especially the large river-dominated coastal seas, will become more complex. This is worth attracting more research attention.

4. Concluding remarks

This study reports field observations of surface water pCO_2 and air-sea CO_2 fluxes in the East China Sea off the Changjiang estuary, finding that it was a CO_2 source during the dry and hot summer conditions of August 2023, contrary to it generally being a CO_2 sink during summer. Changjiang discharge plays a key role in causing the CO_2 sink/source conversion on the East China Sea shelf; the decreased flows in August 2023 lowered phytoplankton uptake of CO_2 and increased surface water pCO_2. Additionally, the relatively higher SSTs compared to previous years further elevated the surface water pCO_2. The combined effects of a summer drought and high temperatures in August 2023 turned the East China Sea off the Changjiang estuary from a CO_2 sink to a CO_2 source. In the context of global change, the CO_2 sink or source patterns of the coastal seas, especially the large river-dominated coastal seas, are becoming more complex and need additional studies.

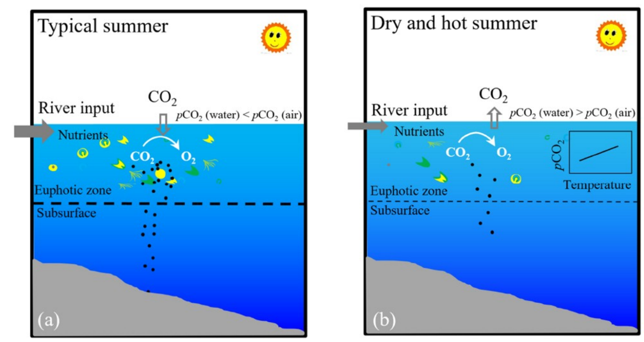

Figure 10 Conceptual model showing reduced freshwater discharge from the Changjiang and high temperatures turned the East China Sea shelf off the Changjiang estuary from a CO_2 sink to a CO_2 source. (a) Status under average river discharge; (b) status under decreased freshwater discharge and higher temperatures. The yellow symbols and black dots denote phytoplankton and particulate organic matter in the water column, respectively. The thick and thin dashed lines represent strong stratification and weak stratification, respectively.

Acknowledgements *We thank the crews of R/V Yanping II for their assistance during the cruise. Chief scientist Dr. Jinyu YANG is appreciated for help during the cruise. Comments and constructive suggestions from reviewers improved the quality of the paper substantially. Richard SMITH is appreciated for English editing. The work was supported by the National Natural Science Foundation of China (Grant Nos. 42141001, 42188102), the National Key R&D Projects (Grant No. 2022YFC3105302) and the Strategic Priority Research Program of the Chinese Academy of Sciences (Grant No. XDB42000000).*

Conflict of interest The authors declare that they have no conflict of interest.

References

Benson B B, Krause Jr. D. 1984. The concentration and isotopic fractionation of oxygen dissolved in freshwater and seawater in equilibrium with the atmosphere. Limnol Oceanogr, 29: 620–632
Carpenter J H. 1965. The Chesapeake Bay Institute technique for the Winkler dissolved oxygen method. Limnol Oceanogr, 10: 141–143
Chen C T A, Wang S L. 1999. Carbon, alkalinity and nutrient budgets on the East China Sea continental shelf. J Geophys Res, 104: 20675–20686
Chou W C, Gong G C, Sheu D D, Jan S, Hung C C, Chen C C. 2009. Reconciling the paradox that the heterotrophic waters of the East China Sea shelf act as a significant CO_2 sink during the summertime: Evidence and implications. Geophys Res Lett, 36: L15607
Chou W C, Gong G C, Tseng C M, Sheu D D, Hung C C, Chang L P, Wang L W. 2011. The carbonate system in the East China Sea in winter. Mar Chem, 123: 44–55
Dai A G, Trenberth K E. 2002. Estimates of freshwater discharge from continents: Latitudinal and seasonal variations. J Hydrometeorol, 3: 660–687

Dai M H, Su J Z, Zhao Y Y, Hofmann E E, Cao Z M, Cai W J, Gan J P, Lacroix F, Laruelle G G, Meng F F, Müller J D, Regnier P A G, Wang G, Wang Z. 2022. Carbon fluxes in the coastal ocean: Synthesis, boundary processes, and future trends. Annu Rev Earth Planet Sci, 50: 593–626

Fassbender A J, Rodgers K B, Palevsky H I, Sabine C L. 2018. Seasonal asymmetry in the evolution of surface ocean $p\mathrm{CO_2}$ and pH thermodynamic drivers and the influence on sea-air CO_2 flux. Glob Biogeochem Cycle, 32: 1476–1497

Gao L, Li D J, Ding P X. 2009. Quasi-simultaneous observation of currents, salinity and nutrients in the Changjiang (Yangtze River) plume on the tidal timescale. J Mar Syst, 75: 265–279

Gao L, Li D, Zhang Y. 2012. Nutrients and particulate organic matter discharged by the Changjiang (Yangtze River): Seasonal variations and temporal trends. J Geophys Res, 117: G04001

Gong G C, Liu K K, Chiang K P, Hsiung T M, Chang J, Chen C C, Hung C C, Chou W C, Chung C C, Chen H Y, Shiah F K, Tsai A Y, Hsieh C H, Shiao J C, Tseng C M, Hsu S C, Lee H J, Lee M A, Lin I I, Tsai F. 2011. Yangtze River floods enhance coastal ocean phytoplankton biomass and potential fish production. Geophys Res Lett, 38: L13603

Guo X H, Zhai W D, Dai M H, Zhang C, Bai Y, Xu Y, Li Q, Wang G Z. 2015. Air-sea CO_2 fluxes in the East China Sea based on multiple-year underway observations. Biogeosciences, 12: 5495–5514

Guo X H, Yao Z T, Gao Y, Luo Y H, Xu Y, Zhai W D. 2021. Seasonal variability and future projection of ocean acidification on the East China Sea shelf off the Changjiang estuary. Front Mar Sci, 8: 770034

Hales B, Takahashi T, Bandstra L. 2005. Atmospheric CO_2 uptake by a coastal upwelling system. Glob Biogeochem Cycle, 19: GB1009

Hu D X, Yang Z S. 2001. Key processes in the fluxes in the East China Sea (in Chinese). Beijing: Ocean Press. 204

Huang W J, Cai W J, Wang Y C, Lohrenz S E, Murrell M C. 2015. The carbon dioxide system on the Mississippi River-dominated continental shelf in the northern Gulf of Mexico: 1. Distribution and air-sea CO_2 flux. J Geophys Res-Oceans, 120: 1429–1445

Kim D, Choi S H, Shim J H, Kim K H, Kim C H. 2013. Revisiting the seasonal variations of sea-air CO_2 fluxes in the northern East China Sea. Terr Atmos Ocean Sci, 24: 409–419

Labasque T, Chaumery C, Aminot A, Kergoat G. 2004. Spectrophotometric Winkler determination of dissolved oxygen: Re-examination of critical factors and reliability. Mar Chem, 88: 53–60

Laruelle G G, Cai W J, Hu X P, Gruber N, Mackenzie F T, Regnier P. 2018. Continental shelves as a variable but increasing global sink for atmospheric carbon dioxide. Nat Commun, 9: 454

Lee H J, Chao S Y. 2003. A climatological description of circulation in and around the East China Sea. Deep Sea Res Part II, 50: 1065–1084

Lei S P, Bu D Z, Guo X H, Xu Y, Yang Y, An S Q, Li Y, Pang J Y, Zhou K B. 2024. Mitigation of hypoxia and ocean acidification on the inner East China Sea shelf impacted by the 2023 summer drought. Mar Pollut Bull, 207: 116830

Li H M, Tang H J, Shi X Y, Zhang C S, Wang X L. 2014. Increased nutrient loads from the Changjiang (Yangtze) River have led to increased Harmful Algal Blooms. Harmful Algae, 39: 92–101

Liu Z Q, Gan J P, Wu H, Hu J, Cai Z, Deng Y. 2021. Advances on coastal and estuarine circulations around the Changjiang estuary in the recent decades (2000-2020). Front Mar Sci, 8: 615929

Shim J H, Kim D, Kang Y C, Lee J H, Jang S T, Kim C H. 2007. Seasonal variations in $p\mathrm{CO_2}$ and its controlling factors in surface seawater of the northern East China Sea. Cont Shelf Res, 27: 2623–2636

Sweeney C, Gloor E, Jacobson A R, Key R M, McKinley G, Sarmiento J L, Wanninkhof R. 2007. Constraining global air-sea gas exchange for CO_2 with recent bomb ^{14}C measurements. Glob Biogeochem Cycle, 21: GB2015

Takahashi T, Olafsson J, Goddard J G, Chipman D W, Sutherland S C. 1993. Seasonal variation of CO_2 and nutrients in the high-latitude surface oceans: A comparative study. Glob Biogeochem Cycle, 7: 843–878

Tseng C M, Liu K K, Gong G C, Shen P Y, Cai W J. 2011. CO_2 uptake in the East China Sea relying on Changjiang runoff is prone to change. Geophys Res Lett, 38: L24609

Tseng C M, Shen P Y, Liu K K. 2014. Synthesis of observed air-sea CO_2 exchange fluxes in the river-dominated East China Sea and improved estimates of annual and seasonal net mean fluxes. Biogeosciences, 11: 3855–3870

Tsunogai S, Watanabe S, Nakamura J, Ono T, Sato T. 1997. A preliminary study of carbon system in the East China Sea. J Oceanogr, 53: 9–17

Tsunogai S, Watanabe S, Sato T. 1999. Is there a “continental shelf pump” for the absorption of atmospheric CO_2? Tellus B, 51: 701

Wang H, Yan H, Zhou F, Li B, Zhuang W, Yang Y. 2019. Dynamics of nutrient export from the Yangtze River to the East China Sea. Estuar Coast Shelf Sci, 229: 106415

Wang S L, Chen C T A, Hong G H, Chung C S. 2000. Carbon dioxide and related parameters in the East China Sea. Cont Shelf Res, 20: 525–544

Wang Z H A, Wanninkhof R, Cai W J, Byrne R H, Hu X P, Peng T H, Huang W J. 2013. The marine inorganic carbon system along the Gulf of Mexico and Atlantic coasts of the United States: Insights from a transregional coastal carbon study. Limnol Oceanogr, 58: 325–342

Wanninkhof R. 1992. Relationship between wind speed and gas exchange over the ocean. J Geophys Res, 97: 7373–7382

Weiss R F. 1974. Carbon dioxide in water and seawater: The solubility of a non-ideal gas. Mar Chem, 2: 203–215

Weiss R F, Price B A. 1980. Nitrous oxide solubility in water and seawater. Mar Chem, 8: 347–359

Wu Y X, Dai M H, Guo X H, Chen J S, Xu Y, Dong X, Dai J W, Zhang Z R. 2021. High-frequency time-series autonomous observations of sea surface $p\mathrm{CO_2}$ and pH. Limnol Oceanogr, 66: 588–606

Yang D, Yin B, Liu Z, Feng X. 2011. Numerical study of the ocean circulation on the East China Sea shelf and a Kuroshio bottom branch northeast of Taiwan in summer. J Geophys Res, 116: C05015

Yu S J, Song Z G, Bai Y, Guo X H, He X Q, Zhai W D, Zhao H D, Dai M H. 2023. Satellite-estimated air-sea CO_2 fluxes in the Bohai Sea, Yellow Sea, and East China Sea: Patterns and variations during 2003-2019. Sci Total Environ, 904: 166804

Yu S J, Wang Z, Jiang Z, Li T, Ding X, Wei X, Liu D. 2024. Marine heatwave and terrestrial drought reduced CO_2 uptake in the East China Sea in 2022. Remote Sens, 16: 849

Yuan D, Li Y, Wang B, He L, Hirose N. 2017. Coastal circulation in the southwestern Yellow Sea in the summers of 2008 and 2009. Cont Shelf Res, 143: 101–117

Zhai W D, Dai M H. 2009. On the seasonal variation of air-sea CO_2 fluxes in the outer Changjiang (Yangtze River) Estuary, East China Sea. Mar Chem, 117: 2–10

Zhai W D, Dai M H, Cai W J, Wang Y C, Hong H S. 2005. The partial pressure of carbon dioxide and air-sea fluxes in the northern South China Sea in spring, summer and autumn. Mar Chem, 96: 87–97

Zhai W D, Dai M H, Chen B S, Guo X H, Li Q, Shang S L, Zhang C Y, Cai W J, Wang D X. 2013. Seasonal variations of sea-air CO_2 fluxes in the largest tropical marginal sea (South China Sea) based on multiple-year underway measurements. Biogeosciences, 10: 7775–7791

Zhai W D, Guo X H, Bai Y, He X Q, Tang K, Dai M H. 2025. Surface CO_2 partial pressure and air-sea CO_2 flux on the China side of the South Yellow Sea based on multiple-year underway measurements during 2005–2011 and comparison with results for 2011–2018. Prog Oceanogr, 234: 103466

Zhang J, Liu S M, Ren J L, Wu Y, Zhang G L. 2007. Nutrient gradients from the eutrophic Changjiang (Yangtze River) Estuary to the oligotrophic Kuroshio waters and re-evaluation of budgets for the East China Sea Shelf. Prog Oceanogr, 74: 449–478

(Editorial handling: Zhimin JIAN)